An improved model for spherical proton emitters*

Xiao-Yan Zhu,[1,2,†] Wei Gao,[3] Lin-Jing Qi,[4] Jia Liu,[5] Wen-Bin Lin,[1,‡] Xun Chen,[2,§] and Xiao-Hua Li[2,¶]

[1]*School of Mathematics and Physics, University of South China, Hengyang, 421001, China*
[2]*School of Nuclear Science and Technology, University of South China, Hengyang, 421001, China*
[3]*School of Physical Science and Technology, Southwest Jiaotong University, Chengdu, 610031, China*
[4]*Department of Physics and Astronomy, Beijing Normal University , Beijing 100875, China*
[5]*School of Nuclear Science and Technology, Lanzhou University, Lanzhou 730000, China*

In the present work, considering the effect of centrifugal potential on proton radioactivity, we propose an improved model to systematically evaluate the proton radioactivity half-lives of spherical proton emitters. The spectroscopic factor S_p has been considered in half-life calculation, determined by using the relativistic mean field (RMF) theory in conjunction with the BCS method based on the DD-ME2 force. The calculated half-lives can reproduce the experimental data within a factor of 2.4. Furthermore, we extend this improved model to predict proton radioactivity half-lives for possible proton candidates that are energetically allowed or observed but not yet quantified in the latest atomic mass excess NUBASE2020. Meanwhile, the universal decay law (UDL), the new Geiger-Nuttall law (N-GNL) and the phenomenological unified fission model (UFM) are also used for comparison. It is found that these predictions are generally consistent with each other.

Keywords: centrifugal potential · proton radioactivity · half-lives · spectroscopic factor

I. INTRODUCTION

Proton radioactivity is a form of nuclear decay where unstable atomic nuclei emit protons, leading to the generation of a new nuclide. This process represents a limit of nuclear stability, in which nuclei with an excess of protons spontaneously emit them to achieve a more stable state. Jackson *et al.* observed the proton transition from the isomeric state of ^{53}Co to the ground state of ^{52}Fe [1, 2] in 1970, and the first experimental detection of proton emission from the ground state of ^{151}Lu was made in 1981 at the GSI velocity filter SHIP [3]. Subsequent discoveries of proton emissions from $^{147}\mathrm{Tm}$, ^{109}I, and ^{113}Cs were made using catcher foil technology in Munich [4]. In 1984, Hofmann *et al.* detected the decay of $^{147}\mathrm{Tm}$ [5] isomers and ^{150}Lu [6]. The development of radioactive beam technology has continuously revealed odd-Z nuclei far from the β-stability line, making them a focal point in nuclear physics research. To date, about 45 proton emitters with $51 \leq Z \leq 83$ have been discovered, 30 of which are in their ground states, while the others are found in isomeric states [7–13]. Proton emission not only provides important information about the shell structures [14, 15] and interactions between bound and unbound states of proton-rich nuclei [16, 17] but also aids in our understanding of the properties and structure of nuclear matter [18–35], thus becoming a significant area of research in the field of nuclear physics.

Theoretically, proton radioactivity is viewed as a quantum tunneling phenomenon through a potential barrier, and is commonly treated using the Wentzel-Kramers-Brillouin (WKB) method. To more accurately describe proton radioactivity and calculate related physical quantities such as half-life, decay energy, orbital angular momentum and preformation factor (or spectroscopic factor), various theoretical models have now been developed. These include the single folding model [36], the Gamow-like model [37, 38], the generalized liquid drop model [39, 40], the distorted-wave Born approximation [41], the one-parameter model (OPM) [42], the density-dependent M3Y (DDM3Y) effective interaction [43, 44], the Woods-Saxon nuclear potential model [45–47], the phenomenological unified fission model (UFM) [48], the Coulomb and proximity potential model [49, 50], the two-potential approach (TPA) [51–54], the universal decay law (UDL) [15], the new Geiger-Nuttall law (N-GNL) [55], the phenomenological formula with four-parameter [56] and so on [57–61]. Utilizing these theoretical methods can enhance our understanding of the phenomenon of proton radioactivity.

Recently, Bayrak [62] put forward a phenomenological modified harmonic oscillator potential model (HOPM) for the favored α decay half-lives of even–even, even–odd, even–odd and odd–odd nuclei. Since α decay, cluster radioactivity and proton radioactivity share same physical mechanism, extending HOPM to research on proton radioactivity seems to be a worthwhile topic to explore. Meanwhile, the spectroscopic factor S_p, is an important physical quantity in the calculation of proton radioactivity half-life, is obtained using the RMF method combined with the BCS method in this paper. However, compared with α decay and cluster radioactivity half-life, the effect of centrifugal potential on proton radioactivity half-life cannot be neglected. Therefore, we generalize HOPM and propose an improved model to systematically calculate the proton radioactivity half-lives of spherical nuclei by considering the effect of centrifugal potential. In addition, we extend this improved model to predict the proton radioactivity half-lives of possible candidates. The corresponding predic-

* Supported by the National Natural Science Foundation of China (Grants Nos: 12175100, 11975132 and 12405154), the Construct Program of the Key Discipline in Hunan Province, the Research Foundation of Education Bureau of Hunan Province, China (Grant No. 18A237), the Natural Science Foundation of Hunan Province, China (Grants No. 2018JJ2321), the Innovation Group of Nuclear and Particle Physics in USC, the Opening Project of Cooperative Innovation Center for Nuclear Fuel Cycle Technology and Equipment, University of South China (Grant No. 2019KFZ10).

† Corresponding author, xyzhu0128@163.com
‡ Corresponding author, lwb@usc.edu.cn
§ Corresponding author, chenxun@usc.edu.cn
¶ Corresponding author, lixiaohuaphysics@126.com

tions are in great agreement with other ones.

The structure of this article is organized as follows. Section II gives a brief introduction of the theoretical framework. In Section III, the detailed calculations and discussions are presented. Finally, Section IV provides a concise summary.

II. THEORETICAL FRAMEWORK

A. The half-life for spherical proton emission

The proton radioactivity half-life $T_{1/2}$ can be generally calculated as

$$T_{1/2} = \frac{\hbar\, ln2}{\Gamma} = \frac{ln2}{\lambda}, \tag{1}$$

where $\hbar$ and λ are the reduced Plank and decay constant, respectively. Γ represents the proton radioactivity width including the normalized factor F and penetration probability P. In semiclassical approximation [62], it can be expressed as

$$\Gamma = \frac{\hbar^2}{4\,\mu} S_p\, F\, P, \tag{2}$$

where the reduced mass $\mu = m_p m_d/(m_p + m_d) \approx A_d A_p M_{nuc}/(A_d + A_p)$ with A_d and A_p being the mass of the daughter nucleus and emitted proton, respectively. S_p, the spectroscopic factor of proton emitters, reflects the probability that the orbit occupied by the emitted proton remains unoccupied in the daughter nucleus.

F describes the probability of the emitted proton collision within the inner region, calculated by integrating over this region. It is written as

$$F = \frac{1}{\int_0^{r_1} \frac{1}{2\,k(r)} dr}. \tag{3}$$

Under the semiclassical WKB approximation, the barrier penetrability P is given by $P = exp(-2S)$, where S is the action integral for the proton penetrating the external barrier. It can be expressed as [62]

$$S = \int_{r_1}^{r_2} k(r)\, dr, \tag{4}$$

where $k(r) = \sqrt{\frac{2\mu}{\hbar^2}|V(r) - Q_p|}$ represents the wave number with r being the separation between the centers of the emitted proton and the daughter nucleus. $V(r)$ is the total interaction potential of the emitted proton-daughter nucleus. In Eqs. (3) and (4), the classical turning points are denoted by r_1 and r_2, which satisfy the conditions $V(r_1) = V(r_2) = Q_p$. Q_p denotes the emitted proton released energy, it can be given by [42]

$$Q_p = \Delta M - (\Delta M_d + \Delta M_p) + k(Z^\beta - Z_d^\beta). \tag{5}$$

where the experimental data for the mass excesses ΔM, ΔM_d, and ΔM_p, representing the parent nucleus, daughter nucleus, and emitted proton, respectively, are taken from the most recent atomic mass data NUBASE2020 [63]. $k(Z^\beta - Z_d^\beta)$ represents the screening effect of atomic electrons with Z_d and Z being the proton numbers of daughter and parent nucleus, for $Z \geq 60, k = 8.7\text{eV}, \beta = 2.517$ and for $Z < 60, k = 13.6\text{eV}, \beta = 2.408$ [64].

During proton emission, the total interaction potential $V(r)$ is typically considered for the emitted proton-daughter nucleus system, which includes the nuclear potential $V_N(r)$, Coulomb potential V_c and centrifugal potential V_l. It can be expressed as

$$V(r) = V_N(r) + V_C(r) + V_l(r), \tag{6}$$

In the present work, we generalize the modified harmonic oscillator potential as nuclear potential to study proton radioactivity [62, 65]. It can be written as

$$V_N(r) = -V_0 + V_1\, r^2, \tag{7}$$

where V_0 and V_1 represent the depth and diffusivity of nuclear potential, respectively. In addition, the Coulomb potential V_c is considered as the nucleus-nucleus interaction between the daughter nucleus and emitted proton, distributed over a uniform sphere with radius R. It can be expressed as [66, 67]

$$V_c(r) = \begin{cases} \frac{Z_d e^2}{2R}[3 - \frac{r^2}{R^2}], & r \leq r_1, \\ \frac{Z_d e^2}{r}, & r > r_1, \end{cases} \tag{8}$$

where $e^2 = 1.4399652$ MeV·fm represents the square of the elementary charge of an electron. R denotes the sharp radius, calculated using the semiempirical formula as

$$R = r_0 A_d^{1/3} + R_p, \tag{9}$$

where A_d is the mass numbers of the daughter nucleus. R_p is the proton radius. In this study, we choose $R_p = 0.8409$ fm and $r_0 = 1.14$ fm [68]. For centrifugal potential V_l, it can be written in the Langer form as

$$V_l(r) = \frac{\hbar^2\, l(l+1)}{2\mu r^2}, \tag{10}$$

where l is the orbital angular momentum carried away by the emitted proton, and the minimum angular momentum l_{min} can be obtained by the conservation laws of spin and parity.

As for favored proton radioactivity, the total interaction potential $V(r)$ between the emitted proton and the daughter nucleus can be written as

$$V(r) = \begin{cases} C_0 - V_0 + (V_1 - C_1)r^2, & r \leq r_1, \\ \frac{C_2}{r}, & r > r_1, \end{cases} \tag{11}$$

where $C_0 = \frac{3Z_d\, e^2}{2R}$, $C_1 = \frac{Z_d\, e^2}{2R^3}$ and $C_2 = Z_d e^2$. As an example to intuitively describe the total nuclear potential $V(r)$, take the nucleus ^{155}Ta in Figure 1. Based on the conditions $V(r_1) = V(r_2) = Q_p$, the values of r_1 and r_2 are derived as $r_1 = \sqrt{\frac{Q_p + V_0 - C_0}{V_1 - C_1}}$ and $r_2 = \frac{C_2}{Q_p}$, respectively.

The Bohr-Sommerfeld quantization condition is regarded

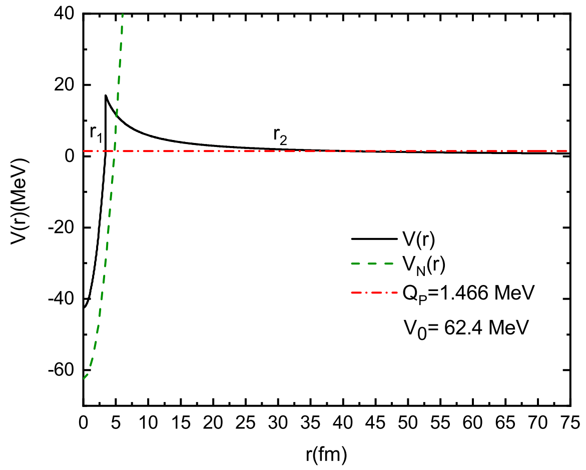

Fig. 1. (color online) The schematic diagram of the total interaction potential $V(r)$ and the modified harmonic oscillator potential $V_N(r)$ versus r.

as an essential part of determining the quantum state in the WKB approximation [52, 69]. In this work, the analytical expression for the nuclear potential diffusivity V_1 is obtained by using Bohr-Sommerfeld quantization condition, which is given by

$$\int_0^{r_1}\sqrt{\frac{2\mu}{\hbar^2}(V(r)-Q_p)}dr=(G-l+1)\frac{\pi}{2}, \tag{12}$$

where $G=2n_r+l$ represents the global principal quantum number with n_r and l being the radial quantum number and the angular momentum quantum number, respectively. For proton radioactivity, we select $G=4$ or 5, corresponding to the $4\hbar\omega$ or $5\hbar\omega$ oscillator shells of the emitted proton. The relationship between V_0 and V_1 can be analytically derived by using the above Eq. (12). It is written as

$$V_1=C_1+\frac{\mu}{2\hbar^2}\left(\frac{Q_p+V_0-C_0}{1+G}\right)^2, \tag{13}$$

with the conditions $C_0<(Q_p+V_0)$ and $C_1<V_1$ need to be satisfied. On the basis of Eq. (13), the normalization factor F in Eq. (3) and the action integral S in Eq. (4) can be further analytically written as

$$F=\frac{4}{\pi}\frac{\mu}{\hbar^2}\left(\frac{Q_p+V_0-C_0}{1+G}\right). \tag{14}$$

$$S=\frac{\sqrt{2\mu}}{\hbar}\frac{C_2}{\sqrt{Q_p}}\left(\arccos\left(\sqrt{\frac{Q_p r_1}{C_2}}\right)-\sqrt{\frac{Q_p r_1}{C_2}-\left(\frac{Q_p r_1}{C_2}\right)^2}\right). \tag{15}$$

Consequently, the logarithmic form of the half-life for favored proton emission can be expressed as

$$\log_{10}T_{1/2}=\log_{10}\left(\frac{\pi\,\hbar\,ln2(1+G)}{Q_p+V_0-C_0}\right)+2\log_{10}(e)S. \tag{16}$$

In the contemplation of the process by favored proton radioactivity, should the orbital angular momentum of the proton being emitted be zero, the influence exerted by the centrifugal potential equally becomes null. Nevertheless, during the spherical proton emission, the centrifugal potential engendered by an orbital angular momentum not equal to zero ($l\neq 0$) elevates the height of the potential barrier, thereby affecting the penetration probability and the related decay process. Compared to α decay and cluster radioactivity, the half-life of proton radioactivity exhibits a greater sensitivity to both the decay energy Q_p and orbital angular momentum l. Hence, it is necessary to consider for the impact of the centrifugal potential on the genesis of spherical proton radioactivity. There are typically two methodologies to address the influence of centrifugal potential:one may either directly add the term $d\sqrt{l(l+1)}$ [70, 71] or $dl(l+1)$ [34, 72, 73] into the corresponding models or empirical formulas. In this work, the term $dl(l+1)$ is introduced to consider the effect of centrifugal potential on the spherical proton emission in Eq. (16). Therefore, an improved model for the half-life of spherical proton emitter is expressed as

$$\log_{10}T_{1/2}=\log_{10}\left(\frac{\pi\,\hbar\,ln2(1+G)}{Q_p+V_0-C_0}\right)+2\log_{10}(e)S+d\,l\,(l+1). \tag{17}$$

B. The spectroscopic factor of proton radioactivity

It is assumed that the core nucleus remains unaltered throughout the decay process. In this study, the spectroscopic factor of the emitted proton-daughter system, S_p, is obtained from the RMF theory and the BCS method [41, 74]. The RMF theory is particularly well suited to investigating the single particle structure of rich proton nuclei based on the Dirac-Lagrangian density, as it naturally incorporates the spin degree of freedom [43, 44]. It can be estimated by

$$S_p^{\rm cal}=u_j^2, \tag{18}$$

where u_j^2 represents the probability that the orbit of the emitted proton is empty in the daughter nucleus. In this work, the nuclear pairing correlations is processed by using the BCS method, the pairing gap for proton and neutron is expressed as a function of the mass number A, i.e., $\Delta n=\Delta p=11.2\,A^{-1/2}$MeV [44].

III. RESULTS AND DISCUSSION

In our previous study [75], we systematically described the cluster radioactivity half-lives by considering the preformation probability based on the HOPM. Given that cluster radioactivity shares the same mechanism with proton radioactivity, we attempt to generalize this model to study the half-lives of spherical proton emissions. It is worth noting that the proton radioactivity half-life is more sensitive to orbital angular momentum than cluster radioactivity [76]. As a consequence, in this work, considering the spectroscopic factor S_p and the effect of the centrifugal potential, we propose an improved model to evaluate the proton radioactivity half-lives for spherical nuclei.

The spectroscopic factor S_p of proton radioactivity, which involves a variety of nuclear structure properties, is also called the formation probability and is crucial in half-life calculation. Some semi-microscopic and the phenomenological methods are used to calculate the spectroscopic factor of proton radioactivity [41, 44, 65, 74, 77, 78]. In this work, the spectroscopic factor S_p is obtained

by using the RMF theory and BCS method with the force parameter chosen as DD-ME2 in Eq. (18), which has demonstrated widespread success and applicability in depicting diverse structural characteristics across a broad spectrum of nuclei [43, 44, 77, 78]. The spectroscopic factor for spherical nuclei are given in the fifth column of Table 1, denoted as $S_p^{\rm cal}$. Delion [65] recently introduced a universal formula that connects the logarithm of the reduced width squared to the fragmentation potential V_{frag}. It was found that the relationship between the spectroscopic factor and the mass of the emitted proton can be well explained by the fragmentation potential V_{frag}, which is given by the difference between the Coulomb barrier V_c and released energy Q_p. It can be written as

$$V_{frag} = \frac{Z_d\, e^2}{r_1} - Q_p. \tag{19}$$

As a means verification, we plot the logarithm of the spectroscopic factor $S_p^{\rm cal}$ for spherical nuclei calculated by Eq. (18) versus the fragmentation potential V_{frag} in Fig. 2. From this figure, one can see that there is a distinct linear relationship between $S_p^{\rm cal}$ and V_{frag} for each class of the orbital angular momentum l. This further substantiates that the spectroscopic factor of proton radioactivity can be accurately described by the RMF theory combine with the BCS method in this work.

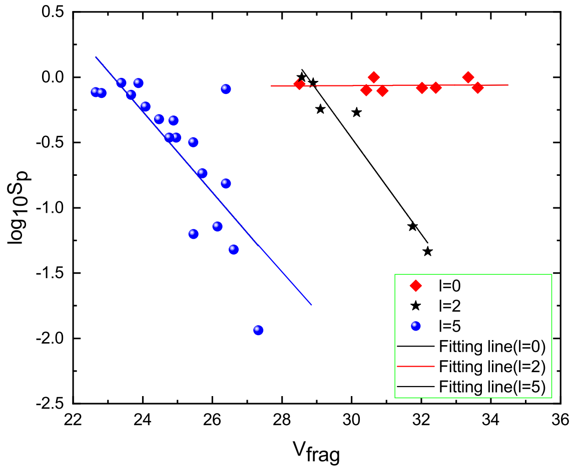

Fig. 2. (color online) The linear relationship between the logarithm of spectroscopic factors $S_p^{\rm cal}$ calculated by Eq. (18) and the fragmentation potential V_{frag}.

With the above confirmation of the reliability of the spectroscopic factors, then based on the S_p values obtained from Eq. (18), we determine the adjustable parameter $V_0 = 62.4$ MeV in Eq. (16) by fitting the experimental half-lives of favored proton emissions. For spherical proton emissions, we directly introduce the term $dl(l+1)$ in Eq. (16) to consider this effect of the centrifugal potential, as shown in Eq.(17). By fitting experimental proton radioactivity half-lives of spherical nuclei, which are taken from the latest nuclear property table NUBASE2020, we obtain the adjustable parameter d in Eq. (17) as $d = 0.143$. Based on the obtained adjustable parameters V_0 and d, the differences Δ between the experimental data of proton radioactivity half-lives and the calculated ones by Eq. (17) for 32 spherical nuclei in logarithmic form are plotted in Fig. 3, denoted as a black symbols. The red symbols in this figure represent the differences Δ obtained from Eq. (16). As can be seen from the figure, the Δ between the experiment data and calculated ones by Eq. (16) for some nuclei become large. In particular, when $l = 5$, the calculated ones are nearly 6 orders of magnitude smaller than experimental data. Therefore, the effect of the centrifugal potential on the proton radioactivity cannot be ignored with the increase of l. The aim of this work is also to generalize the HOPM Eq. (16) to spherical proton emission and to propose an improved model for proton radioactivity half-lives. The differences Δ between the experimental proton radioactivity half-lives and the calculated one in logarithmic form can be expressed as

$$\Delta = \log_{10} T_{1/2}^{\rm exp} - \log_{10} T_{1/2}^{\rm cal}, \tag{20}$$

where $\log_{10} T_{1/2}^{\rm exp}$ and $\log_{10} T_{1/2}^{\rm cal}$ are denote the logarithmic form of experimental half-life and calculated ones, respectively.

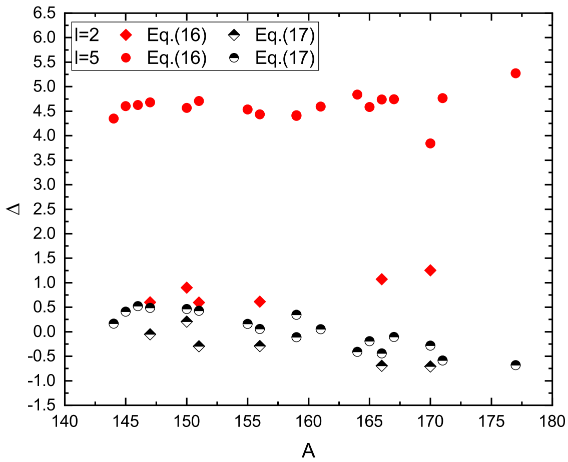

Fig. 3. (color online) The logarithmic differences between experimental half-lives and calculate ones for unfavored proton radioactivity. The different colors represent the different angular momentum taken away by the proton emitters. For each angular momentum cases, the squares and circles are represented by Eq. (16), while the pentagrams and triangles are denoted by Eq. (17), respectively.

In the following, based on the obtained parameters V_0 and d, we systematically calculate the proton radioactivity half-lives of spherical nuclei by using Eq. (17) with the spectroscopic factors taken from Eq. (18). For comparison, UDL [15], N-GNL [55], UFM [48] are also used. The detailed calculations are listed in Table 1. In this table, the first four column provide the proton emission, the released energy Q_p, the spin and parity transition ($j_p^\pi \to j_d^\pi$), and the angular momentum l carried away by the emitted proton, respectively. The middle one column list the calculated spectroscopic factor $S_p^{\rm cal}$ by Eq.(18), The last five columns give the logarithmic form of the experimental proton emissions half-lives and calculated ones using Eq. (17) with S_p obtained by Eq. (18), UDL [15], N-GNL [55], and UFM [48], which expressed as $\log_{10} T_{1/2}^{\rm Exp}$, $\log_{10} T_{1/2}^{\rm Cal}$, $\log_{10} T_{1/2}^{\rm UDL}$, $\log_{10} T_{1/2}^{\rm N-GNL}$ and $\log_{10} T_{1/2}^{\rm UFM}$, respectively. As can be seen from Table 1, compared to other results, the calculated proton radioactivity half-lives $\log_{10} T_{1/2}^{\rm Cal}$ with the obtained spectroscopic factors by Eq. (18) can better reproduce the experimental data except for a few nuclei such as ^{166}Ir$^{\rm m}$, ^{170}Au and ^{177}Tl$^{\rm m}$. It can be found that the

spectroscopic factors S_p are quite small when these daughter nuclei are close to the proton layer. This may be due to the different selection of pairing energy gaps and the number of the basis states used in the calculation. For more visualization, the differences Δ between the experimental half-lives of proton radioactivity and calculated ones, $\log_{10}T_{1/2}^{\mathrm{Cal}}$, $\log_{10}T_{1/2}^{\mathrm{UDL}}$, $\log_{10}T_{1/2}^{\mathrm{N-GNL}}$ and $\log_{10}T_{1/2}^{\mathrm{UFM}}$, are shown in Fig. 4 respectively denoted as the black balls, green pentagrams, red squares and blue upper triangles. From this figure, one can clearly see that $\log_{10}T_{1/2}^{\mathrm{Cal}}$ can reproduce experimental data within the range of $\Delta = \pm 0.4$. It also explains the feasibility of obtaining S_p for spherical proton radioactivity from Eq. (18), and verifies the reliability of the improved model Eq. (17) by considering the effect of centrifugal potential.

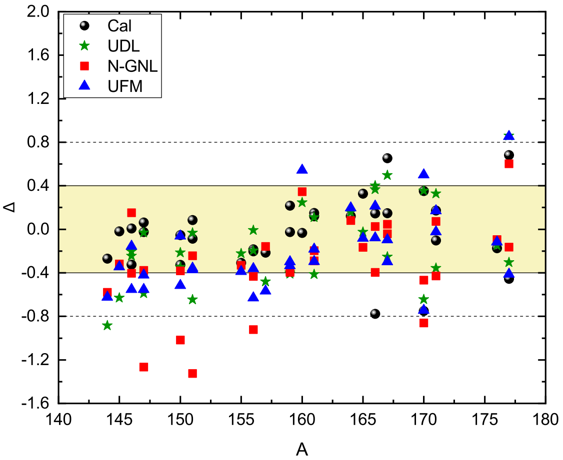

Fig. 4. (color online) Deviations between the theoretical proton radioactivity half-lives and the experimental ones.

Furthermore, the standard deviation σ is used to globally quantify the agreement between experimental data and calculated ones. In this work, σ is defined as

$$\sigma = \sqrt{\frac{1}{n}\sum_{i=1}^{n}\left(\log_{10}T_{i,1/2}^{\mathrm{exp}} - \log_{10}T_{i,1/2}^{\mathrm{cal}}\right)^2}, \tag{21}$$

where $\log_{10}T_{i,1/2}^{\mathrm{cal}}$ and $\log_{10}T_{i,1/2}^{\mathrm{exp}}$ represent the logarithmic form of calculated proton radioactivity half-life and the experimental ones for the i-th nucleus, respectively. As shown in Table 2, σ_{Cal} is only 0.380, which is smaller than all other results. This further indicates that our proposed improved model, which considers the effect of the centrifugal potential, is quite reliable and that considering the spectroscopic factor is also necessary.

In view of the above results calculated are better by Eq. (17), we further extend this model to predict proton radioactivity half-lives for possible candidates, which are energetically allowed or observed but not yet quantified in NUBASE2020. Similarly, we also used UDL[15], N-GNL [55] and UFM [48] for comparison. The detailed predictions are given in table 3, where the first three columns list the proton emitter, the released energy Q_p and the angular momentum l. The last four columns give the predicted proton radioactivity half-lives in logarithmic form using Eq. (17), UDL, N-GNL and UFM respectively. It can be seen from the table that the predictions using our model are relatively consistent with the results of the other two models and/or formulas, and in particular with the UFM. In addition, to further verify the credibility of our predictions, we plot the relationship between the logarithmic values of predicted proton radioactivity half-lives by Eq. (17), UDL, N-GNL and UFM and $(Z_d^{0.8}+l)+Q_p^{-1/2}$ of the new Geiger-Nuttall law [55]. As shown in Fig. 5 (a), (b), (c) and (d), all predicted proton radioactive half-lives exhibit a linear relationship with $(Z_d^{0.8}+l)+Q_p^{-1/2}$, which strongly validates the reliability of our predictions and provides substantial support for future research on the proton radioactivity half-lives of newly synthesized isotopes.

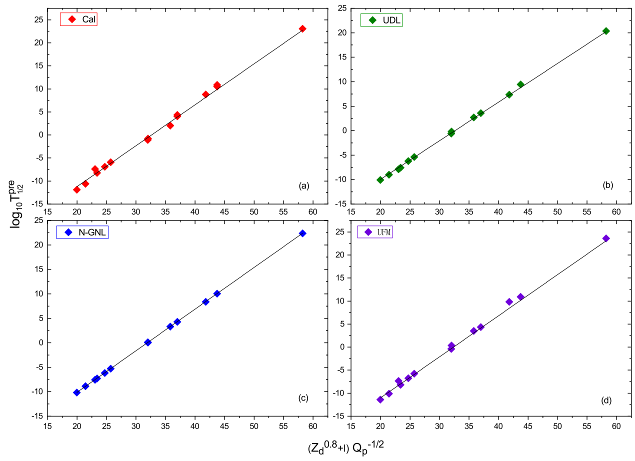

Fig. 5. (color online) Relationship between the predictions of these models and/or formulas given in Table 3 and $(Z_d^{0.8}+l)+Q_p^{-1/2}$.

TABLE 1. Comparison between the experimental and calculated proton radioactivity half-lives for spherical nuclei. The symbol $'\#'$ represents estimated values based on trends in neighboring nuclides with the same Z and N parities. The symbol m denotes the isomeric state, and $'()'$ denotes uncertain spin and/or parity, the experimental data for proton radioactivity half-lives, Q_p values and spin-parity information are obtained from Refs. [34, 38]

Nuclei	Q_p(MeV)	$j_p^x \longrightarrow j_d^x$	l	S_p^{cal}	$\log_{10}T_{1/2}^{\mathrm{Exp}}$	$\log_{10}T_{1/2}^{\mathrm{Cal}}$	$\log_{10}T_{1/2}^{\mathrm{UDL}}$	$\log_{10}T_{1/2}^{\mathrm{N-GNL}}$	$\log_{10}T_{1/2}^{\mathrm{UFM}}$
^{144}Tm	1.724	$(10^+) \rightarrow 9/2^-\#$	5	0.769	-5.569	-5.734	-4.685	-4.989	-4.832
^{145}Tm	1.754	$(11/2^-) \rightarrow 0^+$	5	0.756	-5.499	-5.908	-4.869	-5.180	-5.033
^{146}Tm	0.904	$(1^+) \rightarrow (1/2^+)$	0	0.889	-0.810	-0.975	-0.605	-0.963	-0.603
^{146}Tm^{m}	1.214	$(5^-) \rightarrow (1/2^+)$	5	0.906	-1.137	-1.660	-0.893	-0.733	-0.542
^{147}Tm^{m}	1.133	$3/2^+ \rightarrow 0^+$	2	0.999	-3.444	-3.393	-2.855	-2.179	-3.023
^{147}Tm	1.072	$11/2^- \rightarrow 0^+$	5	0.732	0.587	0.100	0.618	0.965	1.274
^{150}Lu^{m}	1.305	$(1+, 2^+) \rightarrow (1/2^+)$	2	0.901	-4.398	-4.605	-4.050	-3.381	-4.292
^{150}Lu	1.285	$(5^-) \rightarrow (1/2^+)$	5	0.901	-1.347	-1.812	-1.132	-0.965	-0.785
^{151}Lu^{m}	1.315	$3/2^+ \rightarrow 0^+$	2	0.569	-4.796	-4.501	-4.150	-3.472	-4.203
^{151}Lu	1.255	$11/2^- \rightarrow 0^+$	5	0.597	-0.896	-1.322	-0.863	-0.654	-0.300
^{155}Ta	1.466	$11/2^- \rightarrow 0^+$	5	0.477	-2.495	-2.655	-2.272	-2.164	-1.785
^{156}Ta	1.036	$(2^-) \rightarrow 7/2^-\#$	2	0.536	-0.826	-0.537	-0.630	0.096	-0.193
^{156}Ta^{m}	1.126	$(9^+) \rightarrow 7/2^-\#$	5	0.466	0.933	0.875	0.942	1.366	-1.896
^{157}Ta	0.946	$1/2^+ \rightarrow 0^+$	0	0.795	-0.527	-0.171	-0.045	-0.369	-0.140
^{159}Re^{m}	1.816	$11/2^- \rightarrow 0^+$	5	0.344	-4.665	-5.013	-4.267	-4.282	-4.366
^{159}Re	1.816	$11/2^- \rightarrow 0^+$	5	0.344	-4.678	-4.569	-4.268	-4.284	-3.904
^{160}Re	1.267	$(4^-) \rightarrow 7/2^-\#$	0	0.997	-3.163	-3.928	-3.408	-3.508	-3.704
^{161}Re	1.216	$1/2^+ \rightarrow 0^+$	0	0.786	-3.306	-3.247	-2.893	-3.017	-3.020
^{161}Re^{m}	1.336	$11/2^- \rightarrow 0^+$	5	0.317	-0.678	-0.731	-0.788	-0.481	-0.117
^{164}Ir	1.844	$(9^+) \rightarrow 7/2^-$	5	0.063	-3.959	-3.552	-4.114	-4.039	-2.956
^{165}Ir^{m}	1.727	$(11/2^-) \rightarrow 0^+$	5	0.184	-3.433	-3.241	-3.409	-3.267	-2.615
^{166}Ir	1.167	$(2^-) \rightarrow (7/2^-)$	2	0.072	-0.824	-0.131	-1.189	-0.428	-0.105
^{166}Ir^{m}	1.347	$(9^+) \rightarrow (7/2^-)$	5	0.072	-0.076	-0.363	-0.477	-0.102	-1.145
^{167}Ir	1.087	$1/2^+ \rightarrow 0^+$	0	0.828	-1.120	-0.972	-0.867	-1.078	-0.739
^{167}Ir^{m}	1.262	$11/2^- \rightarrow 0^+$	5	0.153	0.842	0.949	-0.346	0.796	-1.753
^{170}Au	1.487	$(2^-) \rightarrow (7/2^-)$	2	0.046	-3.487	-2.779	-3.841	-3.020	-2.650
^{170}Au^{m}	1.767	$(9^+) \rightarrow (7/2^-)$	5	0.811	-3.975	-3.691	-3.331	-3.115	-3.140
^{171}Au	1.464	$1/2^+ \rightarrow 0^+$	0	0.831	-4.652	-4.681	-4.294	-4.224	-4.549
^{171}Au^{m}	1.702	$11/2^- \rightarrow 0^+$	5	0.048	-2.587	-2.000	-2.915	-2.660	-1.439
^{176}Tl	1.278	$(3^-, 4^-) \rightarrow (7/2^-)$	0	0.999	-2.208	-2.254	-2.059	-2.113	-2.091
^{177}Tl	1.173	$(1/2^+) \rightarrow 0^+$	0	0.832	-1.178	-0.863	-0.875	-1.014	-0.687
^{177}Tl^{m}	1.963	$(11/2^-) \rightarrow 0^+$	5	0.012	-3.346	-2666	-4.205	-3.948	-2.278

TABLE 2. The standard deviation σ between the experimental proton radioactivity half-lives and calculated ones obtained using Eq. (17), UDL, N-GNL, UFM.

Models	**Cal**	**UDL**	**N-GNL**	**UFM**
σ	0.380	0.403	0.525	0.705

TABLE 3. Comparison of the predicted proton radioactivity half-lives, which are observed or their proton radioactivity is energetically allowed but not yet quantified in the latest atomic mass excess NUBASE2020 [63] and the related Ref. [34, 38], have been predicted using Eq. (17), UDL, N-GNL, and UFM.

				$\log_{10} T_{1/2}(s)$			
Nuclei	Q_p(MeV)	l	$\mathrm{S_p^{cal}}$	Cal	UDL	N-GNL	UFM
$^{111}\mathrm{Cs}$	1.740	2	0.992	-11.910	-10.094	-10.145	-11.406
$^{116}\mathrm{La}$	1.591	2	0.984	-10.629	-9.000	-8.887	-10.128
$^{127}\mathrm{Pm}$	0.792	2	0.625	-1.063	-0.620	0.094	-0.411
$^{137}\mathrm{Tb}$	0.843	5	0.961	2.023	2.714	3.293	3.490
$^{146}\mathrm{Tm^n}$	1.144	5	0.747	-0.795	-0.177	0.065	0.358
$^{159}\mathrm{Re}$	1.606	0	0.745	-6.892	-6.227	-6.156	-6.735
$^{165}\mathrm{Ir}$	1.547	0	0.786	-5.924	-5.387	-5.303	-5.786
$^{169}\mathrm{Ir^m}$	0.782	5	0.116	8.248	7.362	8.363	9.829
$^{171}\mathrm{Ir^m}$	0.403	5	0.152	23.070	20.337	22.337	23.605
$^{168}\mathrm{Au}$	2.007	0	0.047	-7.376	-7.887	-7.576	-7.326
$^{169}\mathrm{Au}$	1.947	0	0.788	-8.248	-7.572	-7.276	-8.196
$^{172}\mathrm{Au}$	0.877	2	0.998	4.059	3.578	4.284	4.347
$^{172}\mathrm{Au^m}$	0.627	2	0.999	10.530	9.433	10.034	10.921

IV. SUMMARY

In summary, obtaining the spectroscopic factor S_p for proton radioactivity using the RMF method combined with the BCS method, we generalize the HOPM and put forward an improved model to describe the proton radioactivity half-lives for spherical nuclei, considering the effect of centrifugal potential. This improved model contains two adjustable parameters, V_0 and d, which are determined by fitting the experimental proton radioactivity half-lives for spherical nuclei. It is found that the calculated half-lives could accurately reproduce the experimental ones. In addition, we extend this model to predict proton radioactivity half-lives for possible candidates. The corresponding predictions are in quite agreement with other ones obtained by UDL, N-GNL and UFM. It is desired to provide valuable information for further experiments and theory.

REFERENCES

[1] K.P. Jackson, C.U. Cardinal, H.C. Evans et al., $^{53}\mathrm{Co}^{\mathrm{m}}$: A proton-unstable isomer. Phys. Lett. B **33**, 281 (1970). https://doi.org/10.1016/0370-2693(70)90269-8

[2] J. Cerny, J.E. Esterl, R.A. Gough et al., Confirmed proton radioactivity of $^{53}\mathrm{Co}^{\mathrm{m}}$. Phys. Lett. B **33**, 284 (1970). https://doi.org/10.1016/0370-2693(70)90270-4

[3] S. Hofmann, W. Reisdorf, G. Münzenberg et al., Proton radioactivity of $^{151}\mathrm{Lu}$. Z. Phys. A **305**, 111 (1982). https://doi.org/10.1007/BF01415018

[4] T. Faestermann, A. Gillitzer, K. Hartel, et al., Evidence for proton radioactivity of $^{113}\mathrm{Cs}$ and $^{109}\mathrm{I}$. Phys. Lett. B, **137**, 23 (1984). https://doi.org/10.1016/0370-2693(84)91098-0

[5] O. Klepper, T. Batsch, S. Hofmann et al., Direct and beta-delayed proton decay of very neutron-deficient rare-earth isotopes produced in the reaction $^{58}\mathrm{Ni} + {}^{92}\mathrm{Mo}$. Z. Phys. A **305**, 125 (1982). https://doi.org/10.1007/BF01415019

[6] S. Hofmann, in Proceedings of the 7th International Conferbence on Atomic Masses Fundamental Constants, edited by O. Klepper, THD-Schriftenreihe Wissenschaft und Technik Vol.26 (GSI, Darmstadt, 1984), p. 184..

[7] D. Rudolph, C. Andreoiu, C. Fahlander et al., Prompt Proton Decay Scheme of $^{59}\mathrm{Cu}$. Phys. Rev. Lett. **89**, 022501 (2002). https://doi.org/10.1103/PhysRevLett.89.022501

[8] S.Y. Wang, Z.L. Zhu, Z.M. Niu, Influence of the Coulomb exchange term on nuclear single-proton resonances. Nucl. Scie. Tech. **27**, 122 (2016). https://doi.org/10.1007/s41365-016-0125-3

[9] P.J. Sellin, P.J. Woods, T.Davinson et al., Proton spectroscopy beyond the drip line near A= 150. Phys. Rev. C **47**, 1933 (1993). https://doi.org/10.1103/PhysRevC.47.1933

[10] L. Zhou, S.M. Wang, D.Q. Fang et al., Recent progress in two-proton radioactivity. Nucl. Scie. Tech. **33**, 105 (2022). https://doi.org/10.1007/s41365-022-01091-1

[11] R.D. Page, P.J. Woods, R.A. Cunningham et al., Discovery of new proton emitters sup $^{160}\mathrm{Re}$ and $^{156}\mathrm{Ta}$. Phys. Rev. Lett. **68**, 1287 (1992). https://doi.org/10.1103/PhysRevLett.68.1287

[12] H.C. Manjunatha, N. Sowmya, P.S. Damodara Gupta et al., Investigation of decay modes of superheavy nuclei. Nucl. Sci. Tech. **32**, 130 (2021). https://doi.org/10.1007/s41365-021-00967-y

[13] K. Livingston, P.J. Woods, T. Davinson et al., Isomeric proton emission from the drip-line nucleus $^{156}\mathrm{Ta}$. Phys. Rev. C **48**, R2151 (1993). https://doi.org/10.1103/PhysRevC.48.R2151

[14] M. Karny, K.P. Rykaczewski, R.K. Grzywacz et al., Shell structure beyond the proton drip line studied via proton emission from deformed $^{141}\mathrm{Ho}$. Phys. Lett. B **664**, 1 (2008). https://doi.org/10.1016/j.physletb.2008.04.056

[15] C. Qi, D.S. Delion, R.J. Liotta et al., Effects of formation properties in one-proton radioactivity. Phys. Rev. C **85**, 011303 (2012). https://doi.org/10.1103/PhysRevC.85.011303

[16] A.T. Kruppa, W. Nazarewicz, Gamow and R-matrix approach to proton emitting nuclei. Phys. Rev. C **69**, 054311 (2004). https://doi.org/10.1103/PhysRevC.69.054311

[17] G. Gamow, The quantum theory of nuclear disintegration. Nature **122**, 805 (1928). https://doi.org/10.1038/122805b0

[18] L. Zhou, D.Q. Fang, Effect of source size and emission time on the p–p momentum correlation function in the two-proton emission process. Nucl. Scie. Tech. **31**, 52 (2020). https://doi.org/10.1007/s41365-020-00759-w

[19] D.S. Delion, R. J. Liotta, R. Wyss, Systematics of proton emission. Phys. Rev. Lett. **96**, 072501 (2006). https://doi.org/10.1103/PhysRevLett.96.072501

[20] M.H. Zhang, Y.H. Zhang, F.S. Zhang et al., Progress in transport models of heavy-ion collisions for the synthesis of superheavy nuclei. Nucl. Tech. **46**, 080014 (2023). https://doi.org/10.11889/j.0253-3219.2023.hjs.46.080014

[21] M. Li, C.X. Chen, L.F. Xiao et al., Alpha-decay properties of nuclei around neutron magic numbers. Nucl. Scie. Tech. **36**, 14 (2025). https://doi.org/10.1007/s41365-024-01579-y

[22] Q.F. Song, L. Zhu, H. Guo et al., Verification of neutron-induced fission product yields evaluated by a tensor decompsition model in transport-burnup simulations. Nucl. Sci. Tech. **34**, 32 (2023). https://doi.org/10.1007/s41365-023-01176-5

[23] Z. Yuan, D. Bai, Z. Wang et al., Research on two-proton radioactivity in density-dependent cluster model. Sci. China Phys. Mech. Astron. **66**, 222012 (2023). https://doi.org/10.1007/s11433-022-1994-8

[24] D.X. Zhu, Y.Y. Xu, L.J. Chu et al., Two-proton radioactivity from excited states of proton-rich nuclei within Coulomb and Proximity Potential Model. Nucl. Scie. Tech. **34**, 130 (2023). https://doi.org/10.1007/s41365-023-01268-2

[25] M.Q. Ding, D.Q. Fang, Y.G Ma, Neutron skin and its effects in heavy-ion collisions. Nucl. Scie. Tech. **35**, 211 (2024). https://doi.org/10.1007/s41365-024-01584-1

[26] E.B. Huo, T.T. Sun, K.R. Li et al., Continuum Skyrme Hartree–Fock–Bogoliubov theory with Green's function method for neutron-rich Ca, Ni, Zr, Sn isotopes. Nucl. Sci. Tech. **34**, 105 (2022). https://doi.org/10.1007/s41365-023-01261-9

[27] G.F. Wei, X. Huang, Q. Zhi et al., Effects of the momentum dependence of nuclear symmetry potential on pion observables in Sn+Sn collisions at 270 MeV/nucleon. Nucl. Sci. Tech. **33**, 163 (2022). https://doi.org/10.1007/s41365-022-01146-3

[28] M.H. Zhang, Y.H. Zhang, F.S. Zhang et al., Possibilities for the synthesis of superheavy element $Z = 121$ in fusion reactions. Nucl. Sci. Tech. **35**, 95 (2024). https://doi.org/10.1007/s41365-024-01452-y

[29] D.X. Zhu, Y.Y. Xu, H.M. Liu et al., Two-proton radioac-

tivity of the excited state within the Gamowlike and modified Gamow-like models. Nucl. Scie. Tech. **33**, 122 (2022). https://doi.org/10.1007/s41365-022-01116-9

[30] R. Budaca, A. I. Budaca, Proton emission with a screened electrostatic barrier. Eur. Phys. J. A **53**, 1 (2017). https://doi.org/10.1140/epja/i2017-12352-0

[31] X.F. Li, D.Q. Fang, Y.G. Ma, Determination of the neutron skin thickness from interaction cross section and charge-changing cross section for B, C, N, O, F isotopes. Nucl. Sci. Tech. **27**, 71 (2016). https://doi.org/10.1007/s41365-016-0064-z

[32] C. Xu, M. Bao, Improved mass relations of mirror nuclei. Nucl. Scie. Tech. **35**, 157 (2024). https://doi.org/10.1007/s41365-024-01501-6

[33] S. Madhu, H.C. Manjunatha, N. Sowmya et al., Cr induced fusion reactions to synthesize superheavy elements. Nucl. Sci. Tech. **35**, 90 (2024). https://doi.org/10.1007/s41365-024-01449-7

[34] Y.Y. Xu, X.Y. Hu, D.X. Zhu et al., Systematic study of proton radioactivity half-lives. Nucl. Sci. Tech **34**, 30 (2023). https://doi.org/10.1007/s41365-023-01178-3

[35] S.H. Zhu, T.L. Zhao, X.J. Bao, Systematic study of the synthesis of heavy and superheavy nuclei in 48Ca induced fusion evaporation reactions. Nucl. Sci. Tech. **35**, 124 (2024). https://doi.org/10.1007/s41365-024-01483-5

[36] D.N. Basu, P.R. Chowdhury, C. Samanta, Folding model analysis of proton radioactivity of spherical proton emitters. Phys. Rev. C **72**, 051601 (2005). https://doi.org/10.1103/PhysRevC.72.051601

[37] H.M. Liu, X. Pan, Y.T. Zou et al., Systematic study of two-proton radioactivity within a Gamow-like model. Chin. Phys. C **45**, 044110 (2021). https://doi.org/10.1088/1674-1137

[38] D.M. Zhang, L.J. Qi, D.X. Zhu et al., Systematic study on the proton radioactivity of spherical proton emitters. Nucl. Scie. Tech. **34** 55 (2023). https://doi.org/10.1007/s41365-023-01201-7

[39] J. M. Dong, H. F. Zhang, G. Royer, Proton radioactivity within a generalized liquid drop model. Phys. Rev. C **79**, 054330 (2009). https://doi.org/10.1103/PhysRevC.79.054330

[40] Y.Z. Wang, J.P. Cui, Y.L. Zhang et al., Competition between α decay and proton radioactivity of neutron-deficient nuclei. Phys. Rev. C **95**, 014302 (2017). https://doi.org/10.1103/PhysRevC.95.014302

[41] S. Åberg, P.B. Semmes, W. Nazarewicz, Spherical proton emitters. Phys. Rev. C **56**, 1762 (1997). https://doi.org/10.1103/PhysRevC.56.1762

[42] Y.T. Zou, X. Pan, X.H. Li et al., Favored one proton radioactivity within a one-parameter model. Commun. Theor. Phys. **74**, 115302 (2022). https://doi.org/article/10.1088/1572-9494

[43] M. Bhattacharya, G. Gangopadhyay, Microscopic calculation of half lives of spherical proton emitters. Phys. Lett. B **651**, 263 (2007). https://doi.org/10.1016/j.physletb.2007.06.012

[44] Y.B. Qian, Z.Z. Ren, D.D. Ni et al., Half-lives of proton emitters with a deformed density-dependent model. Chin. Phys. Lett. **27**, 112301 (2010). https://doi.org/10.1088/0256-307X/27/11/112301

[45] J. Dudek, Z. Szymański, T. Werner, Woods-Saxon potential parameters optimized to the high spin spectra in the lead region. Phys. Rev. C **23**, 920 (1981). https://doi.org/10.1103/PhysRevC.23.920

[46] S.A. Alavi, V. Dehghani, M. Sayahi, Calculation of proton radioactivity half-lives. Nucl. Phys. A **977**, 49 (2018). https://doi.org/10.1016/j.nuclphysa.2018.06.001

[47] B. Buck, A. C. Merchant, S. M. Perez, Ground state proton emission from heavy nuclei. Phys. Rev. C **45**, 1688 (1992). https://doi.org/10.1103/PhysRevC.45.1688

[48] J.M. Dong, H.F. Zhang, Z. Wei et al., Unified fission model for proton emission. Chin. Phys. C **34**, 182 (2010). https://doi.org/10.1088/1674-1137/34/2/005

[49] K.P. Santhosh, I. Sukumaran, Description of proton radioactivity using the Coulomb and proximity potential model for deformed nuclei. Phys. Rev. C **96**, 034619 (2017). https://doi.org/10.1103/PhysRevC.96.034619

[50] J.G. Deng, X.H. Li, J.L. Chen et al., Systematic study of proton radioactivity of spherical proton emitters within various versions of proximity potential formalisms. Eur. Phys. J. A **55**, 58 (2019). https://doi.org/10.1140/epja/i2019-12728-0

[51] Y.B. Qian, Z.Z. Ren, Calculations on decay rates of various proton emissions. Eur. Phys. J. A **52**, 1 (2016). https://doi.org/10.1140/epja/i2016-16068-3

[52] J.L. Chen, X.H. Li, X.J. Wu et al., Systematic study on proton radioactivity of spherical proton emitters within two-potential approach. Eur. Phys. J. A **57**, 1 (2021).

[53] H.M. Liu, Y.T. Zou, X. Pan et al., Systematic study of two-proton radioactivity half-lives based on a modified Gamow-like mode. Int. J. Mod. Phys. E **30**, 08 (2021). https://doi.org/10.1142/S0218301321500749

[54] X. Pan, Y.T. Zou, B. He et al., Systematic study of two-proton radioactivity half-lives using two-potential approach with different Skyrme interactions. Int. J. Mod. Phys. E **30**, 08 (2021). https://doi.org/10.1142/S0218301322500513

[55] J.L. Chen, J.Y. Xu, J.G. Deng et al., New Geiger-Nuttall law for proton radioactivity. Eur. Phys. J. A **55**, 214 (2019). https://doi.org/10.1140/epja/i2019-12927-7

[56] I. Sreeja, M. Balasubramaniam, An empirical formula for the half-lives of ground state and isomeric state one proton emission. Eur. Phys. J. A **54**, 106 (2018). https://doi.org/10.1140/epja/i2018-12542-2

[57] V. Dehghani, S.A. Alavi, Empirical formulas for proton decay half-lives: Role of nuclear deformation and Q-value. Chin. Phys. C **42**, 104101 (2018). https://doi.org/10.1088/1674-1137/42/10/104101

[58] J.H. Cheng, X. Pan, Y.T. Zou et al., Systematic study of proton radioactivity of spherical proton emitters with Skyrme interactions. Eur. Phys. J. A **56**, 273 (2020). https://doi.org/10.1140/epja/s10050-020-00280-z

[59] D.D. Ni, Z.Z. Ren, New formula of Half-lives for proton emission from spherical and deformed nuclei. continuum **3**, 4 (2012). doi.org/2012-57-1-2/RomJPhys/57/407

[60] I. Sreeja, M. Balasubramaniam, An empirical formula for the half-lives of exotic two-proton emission. Eur. Phys. J. A **55**, 1 (2019). https://doi.org/10.1140/epja/i2019-12694-5

[61] H.F. Zhang, J.M. Dong, Y.Z. Wang et al., Theoretical analysis and new formulae for half-lives of proton emission. Chin. Phys. L **26**, 072301 (2009). https://doi.org/10.1088/0256-307X/26/7/072301

[62] O. Bayrak, A new simple model for the α-decay. J. Phys. G Nucl. Part. Phys. **47**, 025102 (2020). https://doi.org/10.1088/1361-6471

[63] F.G. Kondev, M. Wang, W.J. Huang et al., The NUBASE2020 evaluation of nuclear physics properties. Chin. Phys. C **45**, 030001 (2021). https://doi.org/10.1088/1674-1137

[64] V.Yu. Denisov, H. Ikezoe, α-nucleus potential for α-decay and sub-barrier fusion. Phys. Rev. C **72**, 064613 (2005). https://doi.org/10.1103/PhysRevC.72.064613

[65] D.S. Delion, Universal decay rule for reduced widths. Phys. Rev. C **80**, 024310 (2009).

https://doi.org/10.1103/PhysRevC.80.024310
[66] B. Buck, A.C. Merchant, S.M. Perez, New look at α decay of heavy nuclei. Phys. Rev. Lett. **65**, 2975 (1990). https://doi.org/10.1103/PhysRevLett.65.2975
[67] B. Buck, A.C. Merchant, S.M. Perez, Ground state to ground state alpha decays of heavy even-even nuclei. J. Phys. G Nucl. Part. Phys. **17**, 1223 (1991). https://doi.org/10.1088/0954-3899/17/8/012
[68] J.L. Chen, X.H. Li, J.H. Cheng et al., Systematic study of proton radioactivity based on Gamow-like model with a screened electrostatic barrier. J. Phys. G: Nucl. Part. Phys. textbf46, 065107 (2019). https://doi.org/10.1088/1361-6471/ab1a56
[69] N.G. Kelkar, H.M. Castañeda, Critical view of WKB decay widths. Phys. Rev C textbf76, 064605 (2007). https://doi.org/10.1103/PhysRevC.76.064605 https://doi.org/10.1140/epja/s10050-021-00618-1
[70] A. Soylu, C. Qi, Extended universal decay law formula for the α and cluster decays. Nucl. Phys. A **1013**, 122221 (2021). https://doi.org/10.1016/j.nuclphysa.2021.122221
[71] X.Y. Zhu, S. Luo, W. Gao et al., An improved simple model for α decay half-lives. Chin. Phys. C **48**, 074102 (2024). https://doi.org/10.1088/1674-1137/ad3d4b
[72] Y. Qian, Z. Ren, Unfavored α decay from ground state to ground state in the range $53 \leq Z \leq 91$. Phys. Rev. C **85**, 027306 (2012). https://doi.org/10.1103/PhysRevC.85.027306
[73] J.G. Deng, H.F. Zhang, G. Royer, Improved empirical formula for α-decay half-lives. Phys. Rev. C **101**, 034307 (2020). https://doi.org/10.1103/PhysRevC.101.034307
[74] D.S. Delion, R.J. Liotta, R. Wyss, Theories of proton emission. Phys. Rep. **424**, 113 (2006). https://doi.org/10.1016/j.physrep.2005.11.001
[75] X.Y. Zhu, S. Luo, L.J. Qi et al., Simple model for cluster radioactivity half-lives in trans-lead nuclei. Chin. Phys. C **47**, 114103 (2023). https://doi.org/10.1088/1674-1137/acf48a
[76] A.A. Sonzogni, Proton radioactivity in $Z > 50$ nuclides. Nucl. Data Sheets **95**, 1 (2002). https://doi.org/10.1006/ndsh.2002.0001
[77] Y.T. Rong, Z.H. Tu, S.G. Zhou, New effective interactions for hypernuclei in a density-dependent relativistic mean field model. Phys. Rev. C **104**, 054321 (2021). https://doi.org/10.1103/PhysRevC.104.054321
[78] J.J. Li, W.H. Long, J. Margueron et al., Superheavy magic structures in the relativistic Hartree–Fock–Bogoliubov approach. Phys. Lett. B **732**, 169 (2014). https://doi.org/10.1016/j.physletb.2014.03.031